



Modeling and Validation of 12V Lead-Acid Battery for Stop-Start Technology

2017-01-1211

Published 03/28/2017

SoDuk Lee

US EPA

Jeff Cherry and Michael Safoutin

US Environmental Protection Agency

Joseph McDonald

US EPA

CITATION: Lee, S., Cherry, J., Safoutin, M., and McDonald, J., "Modeling and Validation of 12V Lead-Acid Battery for Stop-Start Technology," SAE Technical Paper 2017-01-1211, 2017, doi:10.4271/2017-01-1211.

Abstract

As part of the Midterm Evaluation of the 2017-2025 Light-duty Vehicle Greenhouse Gas Standards, the U.S. Environmental Protection Agency (EPA) developed simulation models for studying the effectiveness of stop-start technology for reducing CO₂ emissions from light-duty vehicles.

Stop-start technology is widespread in Europe due to high fuel prices and due to stringent EU CO₂ emissions standards beginning in 2012. Stop-start has recently appeared as a standard equipment option on high-volume vehicles like the Chevrolet Malibu, Ford Fusion, Chrysler 200, Jeep Cherokee, and Ram 1500 truck. EPA has included stop-start technology in its assessment of CO₂-reducing technologies available for compliance with the standards. Simulation and modeling of this technology requires a suitable model of the battery.

The introduction of stop-start has stimulated development of 12-volt battery systems capable of providing the enhanced performance and cycle life durability that it requires. Much of this activity has involved advanced lithium-ion chemistries, variations of lead-acid chemistries, such as absorbed-glass-mat (AGM) designs, and lead-carbon formulations.

EPA tested several AGM batteries that are used in OEM start-stop systems. The purpose of this testing was to develop an equivalent circuit model for integration into EPA's ALPHA vehicle simulation model. Testing was performed at the Battery Test Facility (BTF) at the U.S. Environmental Protection Agency (EPA) National Vehicle and Fuel Emissions Laboratory (NVFEL) in Ann Arbor, Michigan. The Duracell batteries referenced are model number SLI49AGM with a rating of 92 Ah and the X2 Power batteries referenced are model

number SLI34-78AGMDP with a rating of 68 Ah. Both batteries are 6 cell 12 volt using AGM technology. For compatibility with the voltage specifications of the BTF equipment, tests were performed on two batteries connected in series (nominal 24 volts).

This paper presents the development and validation of the lead-acid battery model. The battery model is a standard equivalent circuit model with two Resistance-Capacitance (RC) blocks. Resistances and capacitances were calculated using test data from a Duracell 92Ah lead-acid battery which is aftermarket equipment for the Chevrolet Malibu. The lead-acid battery library in the ALPHA model was validated with data obtained from Argonne National Laboratory (ANL) from their chassis dynamometer testing of the 2010 Mazda 3 Hatchback i-Stop [9] and 2010 VW Golf TDI Diesel Bluemotion [10]. The simulated battery voltages, currents, and state of charge (SOC) are in excellent agreement with the vehicle test data on a number of drive schedules.

Introduction

EPA developed the Advanced Light-Duty Powertrain and Hybrid Analysis (ALPHA) tool to model vehicle performance, fuel economy, and greenhouse gas emissions for light-duty conventional and hybrid electric vehicles. EPA uses ALPHA as an in-house research tool to evaluate the efficiency of new advanced technologies. ALPHA shares many similarities with the heavy-duty Greenhouse Gas Emissions Model (GEM) [1] certification tool, with the addition of modeling components specific to light-duty vehicles. ALPHA includes components for simulating hybrid electric vehicles (HEVs), including models for the electric machine, regenerative braking, supervisory control, and battery.

For modeling 12-volt stop-start technology applications, it is necessary to consider battery pack performance, SOC trajectory optimization, power coupling optimization of the electric motor power and engine power, all of which are important to the overall efficiency of the vehicle.

A two-time constant equivalent circuit battery cell model was developed to closely simulate lead-acid battery pack voltage. The estimated voltage was then used to calculate traction motor and generator current by dividing it from motor power. The motor power was calculated by multiplying motor torque and motor speed estimated from vehicle supervisory controls.

A lumped capacitance battery thermal model was developed to capture pack performance by calculating the pack temperature. The battery pack model enables fuel economy and greenhouse gas emissions to be estimated by simulating the effects of battery power density, SOC operating window, discharge and charge power limits, battery pack temperature, battery cell internal resistance, and thermal control strategies.

Battery Pack Model

The Battery Pack Model in ALPHA consists of an equivalent circuit cell model, a battery thermal model, and battery management system controls (BMS). Accurate SOC and discharge and charge power limits are required to precisely estimate available traction motor power and torque.

Equivalent Circuit Cell Model

A two time constant equivalent circuit model [2, 3] was applied to calculate terminal voltages of a lead-acid cell, and 12V battery voltages were calculated by multiplying 6 cells in series within the lead-acid (PbA) battery.

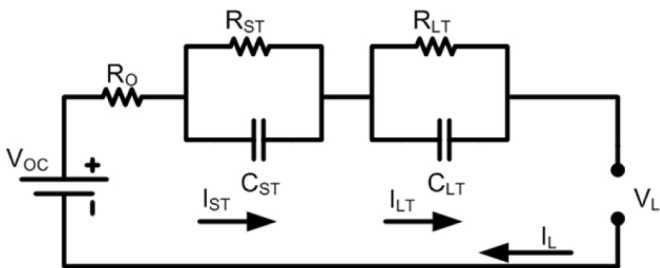


Figure 1. Battery Equivalent Circuit Cell Model

In Figure 1, the V_{oc} as shown in Figure 2 is an open circuit voltage (OCV) of a lead-acid battery cell. R_O is an Ohmic resistance of a battery cell, and is dependent on SOC (state of charge) and cell/pack temperatures. R_{ST} and C_{ST} are resistances and capacitances, respectively, of electro-magnetic short time double layer effects. R_{LT} and C_{LT} are resistances and capacitances of electro-chemical long time mass transport effects. I_L is battery cell load current. Discharge current is positive while charge current is negative.

Battery cell terminal voltage, V_L , can be calculated by using the RC circuit equation (1).

$$V_L = V_{OC} + I_L * R_O + \int (I_L - I_{ST})/C_{ST} dt + \int (I_L - I_{LT})/C_{LT} dt \quad (1)$$

where $I_{ST} = V_{ST}/R_{ST}$ and $I_{LT} = V_{LT}/R_{LT}$.

Equation (1) was implemented by using Matlab/Simulink block diagrams.

Battery pack voltage, V_{Batt} , was calculated by using the following equation.

$$V_{Batt} = V_L * N_{series} / N_{parallel} \quad (2)$$

where N_{series} is 6 cells in series connection and $N_{parallel}$ is 1 for a 12V lead-acid battery.

As shown in Figure 3, averaged Ohmic resistances, short and long time resistances of a 68 Ah X2 Power 12V lead-acid battery [4, 5, 6] were implemented in Matlab/Simulink lookup tables to estimate the effects of SOC and charging/discharging currents.

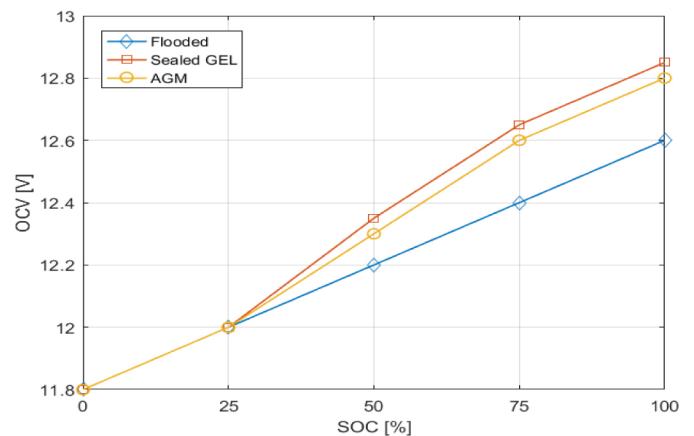


Figure 2. Typical Open Circuit Voltage (OCV) of 12V Lead-Acid Battery

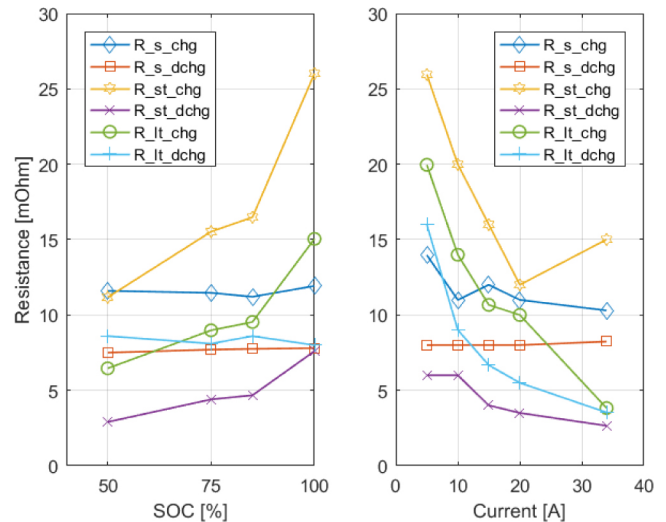


Figure 3. Ohmic, Short and Long Time Resistances of 68Ah 12V X2 Power Lead-Acid Battery

Ohmic resistances in the charging mode (R_{s_chg}) are higher than those in discharge (R_{s_dchg}), as shown in Figure 3. Similarly, RC short time constants in charging (τ_{st_chg}) are higher than those of discharging (τ_{st_dchg}) as shown in Figure 4.

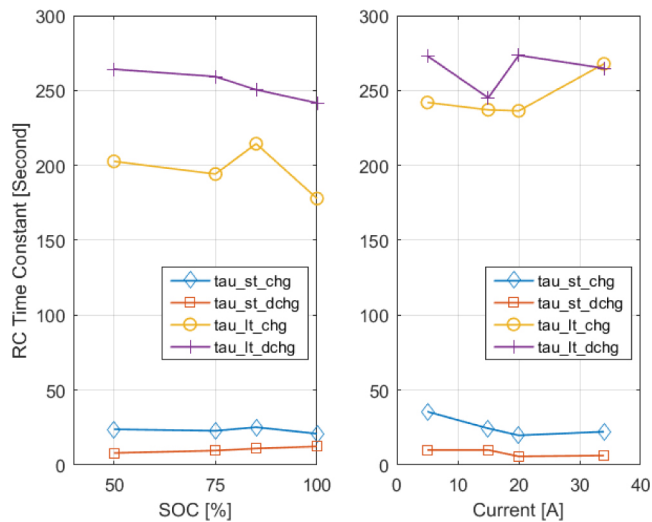


Figure 4. Short and Long Time Constants (τ) of 68Ah 12V X2 Power Lead-Acid Battery

As shown in Figures 5 and 6, the resistances and capacitances of the 92Ah Duracell 12V lead-acid battery were estimated from 10 second charging and discharging current pulse tests to construct Matlab/Simulink lookup tables for the two-time constant equivalent circuit battery model. The resistances and capacitances with respect to SOC and current pulses are presented in the Appendix.

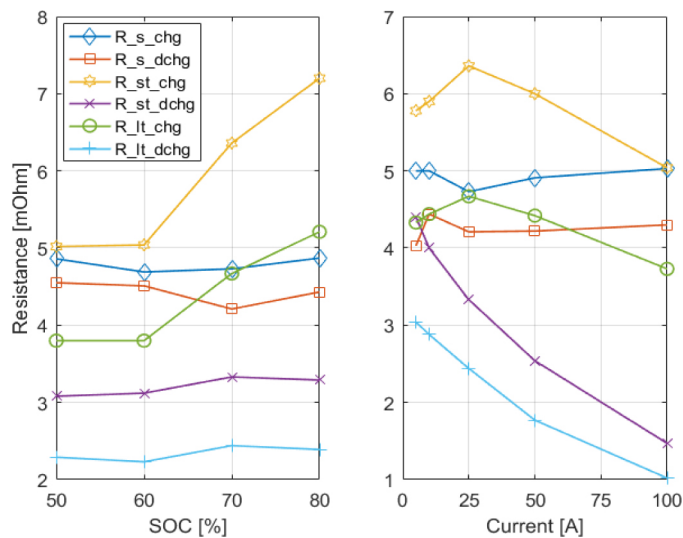


Figure 5. Ohmic, Short and Long Time Resistances of 92Ah 12V Duracell Lead-Acid Battery

Battery pack voltages, V_{Batt} , and battery pack currents, I_L , were obtained from the vehicle CAN communication bus during chassis-dynamometer testing.

In automotive 12V Stop-Start technology applications, the 12V battery experiences high discharging and charging currents. R_{ST} , C_{ST} , R_{LT} and C_{LT} can be calculated by estimating cell voltage recovery response gradients [3] when running high I-V (current-voltage) discharging and charging current pulse tests at various SOC levels. However, voltage response gradients from battery pack I-V tests may be different than those of battery cell I-V tests due to cell-to-cell SOC imbalance, cell-to-cell voltage variations, etc. RC network parameters (R_{ST} , C_{ST} , R_{LT} and C_{LT}) [2] of battery cells were estimated by running I-V pulse tests while discharging less than 1 ampere current.

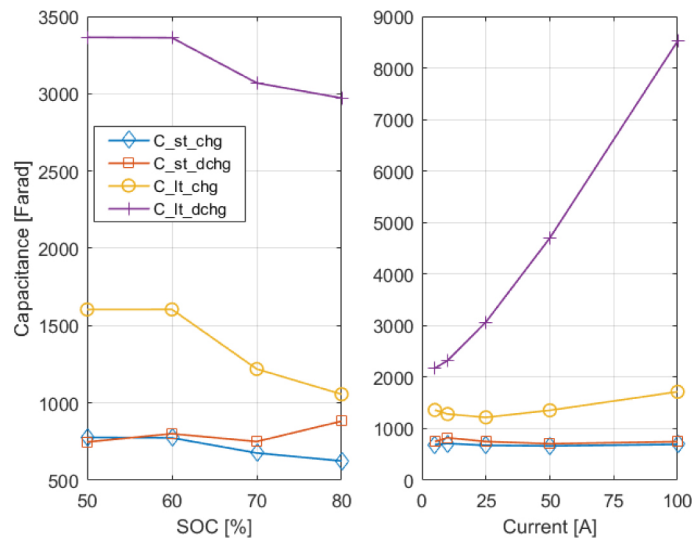


Figure 6. Short and Long Time Capacitances of 92Ah 12V Duracell Lead-Acid Battery

Design of Experiments (DOE) approaches were used to find optimum magnitudes of RC network parameters by using the known values from EPA in-house battery pack test data, the manufacturer's averaged OCV, and V_{Batt} and I_L vehicle CAN values from chassis dynamometer test data. The cost function of this optimization is to find the minimum of RMS battery pack voltage differences in test data and model simulations.

The equations (3), (4), (5), and (6) were calibrated to match RC network parameter values from recent 12V Stop-Start technology lead-acid battery test data [9, 10].

As shown in Figure 7, the simulated battery pack voltages are in good agreement with 12V lead-acid battery test data. The RMS voltage differences between the simulated pack voltage and those of test data are within 0.11 volts. The simulated voltage was quickly recovered by completing the discharging pulse current inputs while the pack voltage of the 12V lead-acid test battery was slowly returned to the open circuit voltage for more than 24 hours of the resting period.

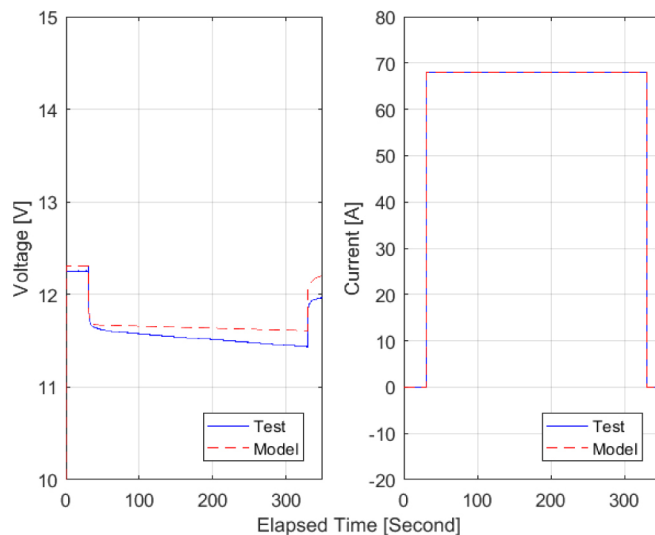


Figure 7. A Discharging Pulse Test at 50% SOC

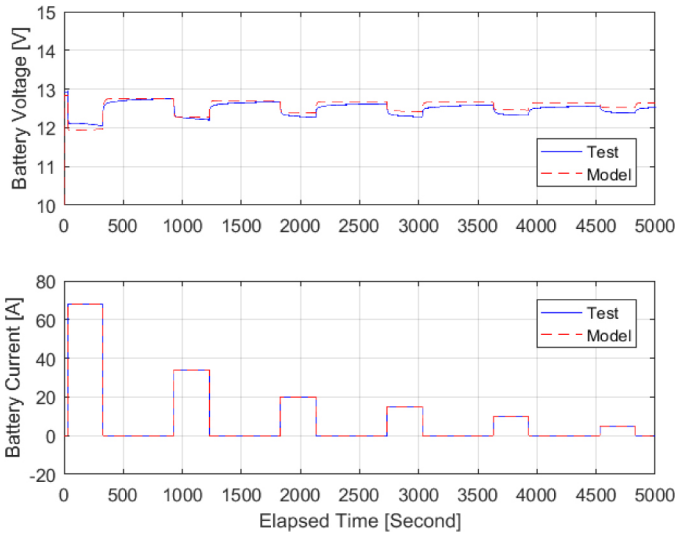


Figure 8. A Series of Discharging Pulse Tests

The RMS voltage differences between the simulated voltages and test data shown in Figure 8 are about 0.8 volts and the simulated voltage averages are within the range of 0.7% of the test data averages.

Battery Thermal Model

The lumped capacitance battery thermal model [5, 6] in ALPHA was developed to feed battery pack temperature information to the battery voltage block, battery power limit control block, and BMS control strategies.

The battery pack temperature was calculated by using the energy balance between battery heat generation, Q_{ees_gen} and heat loss, $Q_{ees_cooling}$, while taking into consideration the thermal mass of the battery pack and the cooling agent.

$$T_{ees} = \int_0^t \frac{(Q_{ees_gen} - Q_{ees_cooling})}{m_{ees} c_{p,ees}} dt + T_0 \quad (3)$$

where m_{ees} is the mass of battery pack, T_0 is the initial pack temperature, and $C_{p,ees}$ is battery heat capacity [7].

The battery heat generation, Q_{ees_gen} is calculated by

$$Q_{ees_gen} = I_L * R_{Batt}^2 + (1 - \text{charge efficiency}) * I_L * V_{Batt} \quad (4)$$

The battery pack resistance, R_{Batt} , is obtained by

$$R_{Batt} = (R_O + R_{ST} * I_{ST}/I_L + R_{LT} * I_{LT}/I_L) * N_{series} / N_{parallel} \quad (5)$$

where R_O is battery cell discharging or charging resistance. The cell resistance, R_O , is estimated by using a 2-dimensional discharging look-up table when battery current is positive, and by using the charging resistance for negative battery current.

The battery heat loss, $Q_{ees_cooling}$, is calculated by

$$Q_{ees_cooling} = (h A_s + kt)(T_{ees} - T_{coolant}) \quad (6)$$

where $T_{coolant}$ is battery pack inlet coolant temperature which, depending on pack configuration can be the temperature of ambient air, cabin-conditioned air or liquid water coolant. A_s is the battery surface area for convection heat transfer and t is the thickness of the battery pack for heat transfer via conduction. A typical battery conduction coefficient, k , and convection coefficient, h , are found in references [6]. The thermal equations were implemented by using Matlab/Simulink blocks. An alternative approach [8] to the battery thermal issue is presented.



Figure 9. Battery Test Setup at EPA NVFEL Battery Test Facility

MODEL SIMULATION

2010 Mazda 3 i-Stop and 2010 Golf TDI Stop-Start battery test data [9] from Argonne National Laboratory were used to validate the lead-acid battery model. The simulated battery voltages and ANL test data voltages were compared while supplying the ANL battery test data currents to the model. In the 2010 Mazda 3 i-Stop, the main 36Ah lead-acid battery is used for powering vehicle controls, lights, spark ignition, etc., and the 12V starter motor uses a separate 21Ah lead-acid battery for enabling the stop-start technology.

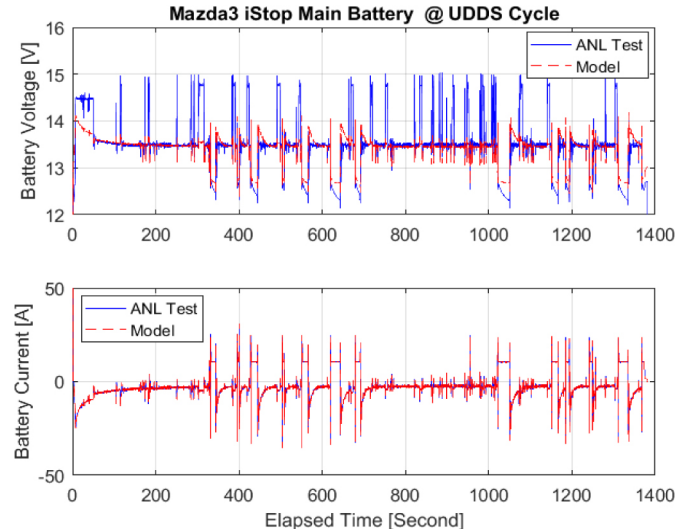


Figure 10. 2010 Mazda3 i-Stop 36Ah Main Battery Voltages

The main battery voltages by model simulations were compared with those of ANL test data. The higher voltage spikes in ANL test data shown in Figure 10 were discovered without any noticeable charging current inputs. Hence, the ANL battery voltage may not be measured at the battery terminals. The 13.41V simulated RMS voltages and 13.48V ANL RMS voltages are in an excellent agreement even though there are some voltage spikes in ANL test data [9].

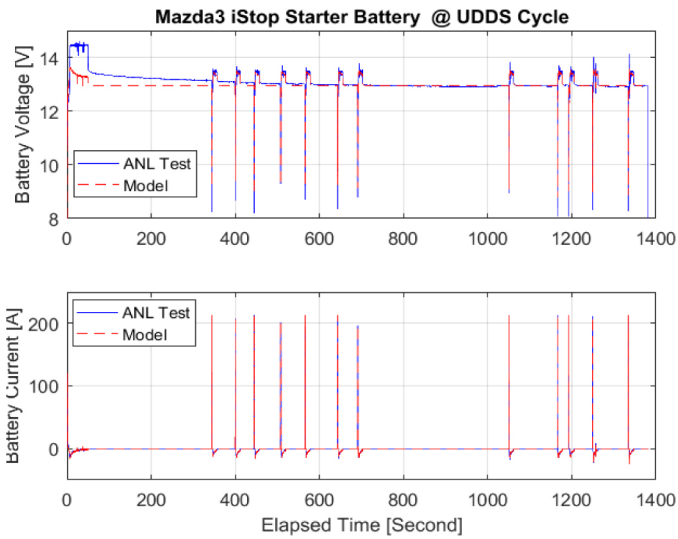


Figure 11. UDDS Cycle Battery Voltage Simulations of the 2010 Mazda3 i-Stop 21Ah 12V Starter lead-acid Battery

As shown in Figure 11, the simulated battery voltages are in good agreement with the pack voltage of the 2010 Mazda3 i-Stop 21Ah lead-acid starter battery data from UDDS cycle chassis-dynamometer ANL tests. The 12.99V simulated RMS voltages are within 0.8% of the 13.09V RMS voltages of ANL 21Ah starter battery test data although there are the higher charging voltages that are maintained at more than 14V without any significant charging current inputs at the beginning of the UDDS cycle test period.

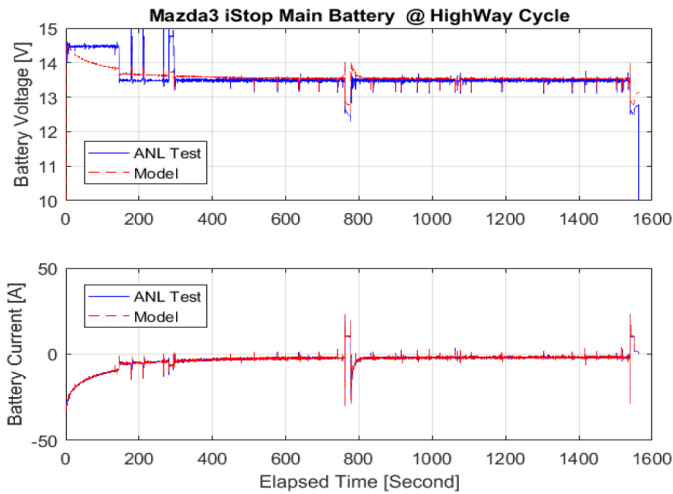


Figure 12. FTP HWFET Cycle Battery Voltage Simulations of the 2010 Mazda3 i-Stop 36Ah Main lead-acid Battery

The 13.59V simulated RMS voltages shown in Figure 12 are also in good agreement with the 13.57V RMS voltage of the 2010 Mazda3 i-Stop 36Ah main battery test data from the FTP High Way Fuel Economy Test (HWFET) cycle chassis-dynamometer ANL tests. The square type charging current inputs are required to maintain the constant higher charging voltages observed in the beginning of the test period. Hence, the battery voltage may not be measured at the battery terminals since the parabolic type charging currents were supplied in the ANL battery test data.

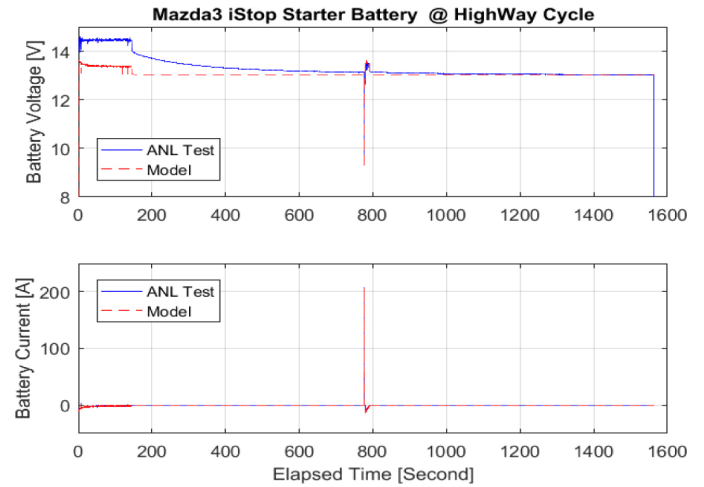


Figure 13. FTP HWFET Cycle Battery Voltage Simulations of the 2010 Mazda3 i-Stop 21Ah lead-acid Starter Battery

The 13.08V simulated RMS voltages are within 1.73% of the 13.31V RMS voltages of ANL test data shown in Figure 13. The ANL battery voltages may be measured at the alternator since 14.5V voltages are typical voltages of the alternator output, and the alternator generated currents may be distributed to 36Ah main battery and 21Ah starter battery [9] simultaneously. The battery voltages slowly return to the open circuit voltage (OCV) level when at rest. However, the simulated battery voltages in the RC circuit will be the same as the OCVs when cutting the external battery currents. Hence, a voltage calibration factor in this lead-acid battery model was implemented to compensate for the slow voltage drops to the OCV level.

Figure 15 shows that the 13.44V simulated RMS voltages are within 0.85% of the 13.33V RMS voltages of ANL test data. There are about 0.5V voltage differences during 10A current discharging from the end of the first US06 cycle to the beginning of the second US06 cycle. The 10A discharging currents may provide enough power for vehicle controls, cabin comfort, etc. without running an internal combustion engine to extend the stop period for better off-cycle technology effectiveness. As shown in Figure 16, the 13.05V simulated RMS voltages are almost identical to the 13.03V RMS voltages of 2010 Mazda 3 i-Stop 21Ah starter battery ANL test data from two US06 driving cycles.

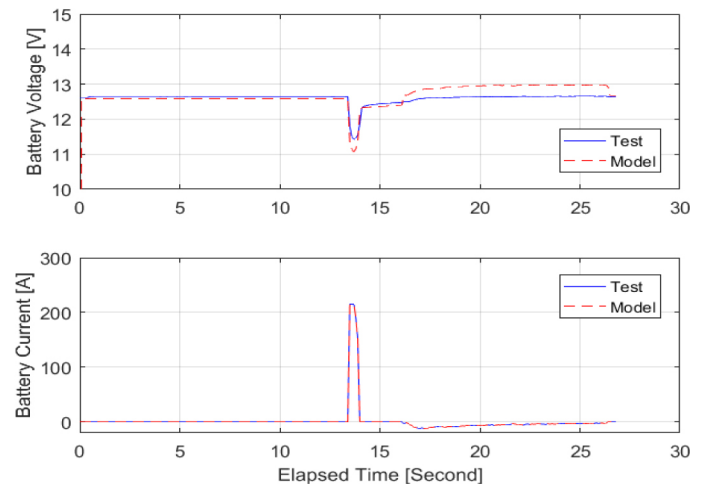


Figure 14. Start-Up Voltage of 2010 Mazda3 i-Stop 21Ah Starter Battery

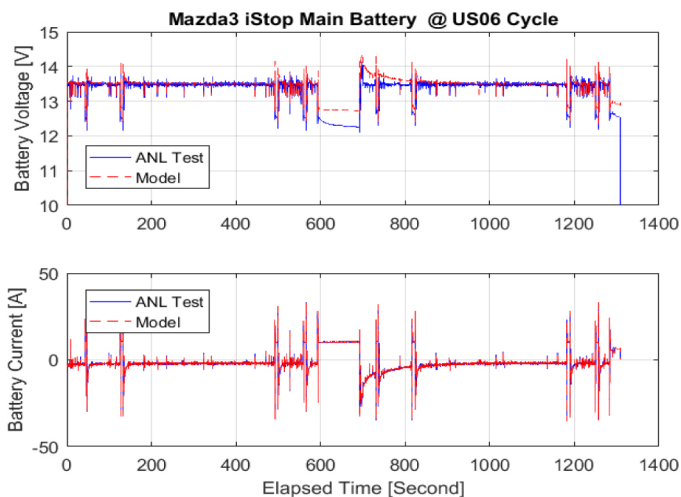


Figure 15. 2010 Mazda3 i-Stop 36Ah Battery Voltages @ 2x US06 cycle

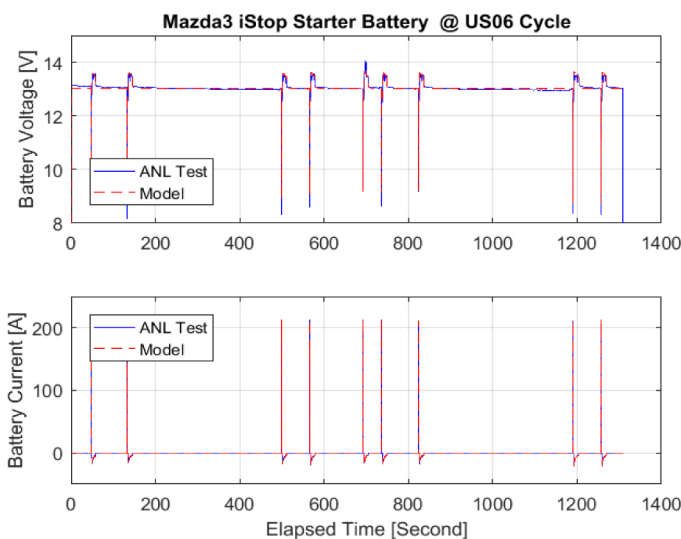


Figure 16. 2010 Mazda3 i-Stop 21Ah Battery Voltages @ 2x US06 cycle

2010 Golf TDI Stop-Start battery current and power test profiles [10] from Argonne National Laboratory were used to validate the 92Ah 12V Duracell lead-acid battery test data. VW UDDS, highway and US06 drive cycle tests as shown in Figure 17, 18 and 19 were conducted at the US EPA NVFEL Battery Test Facility (BTF).

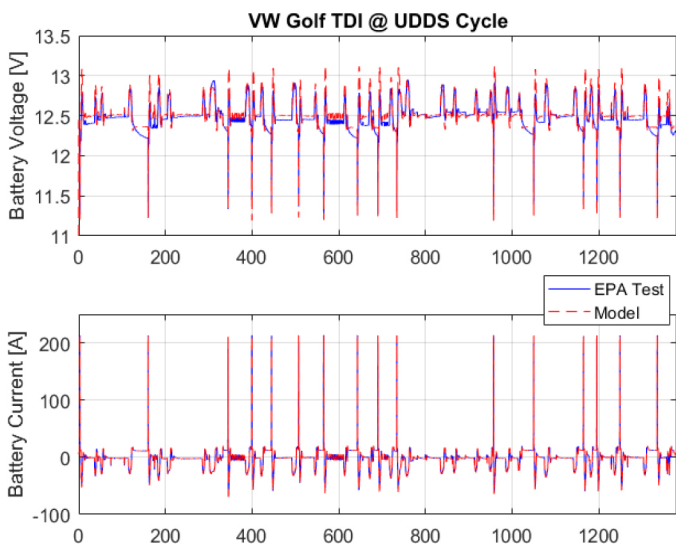


Figure 17. 2010 VW Golf TDI UDDS Cycle Battery Voltages

Figure 17 shows that the 12.52V simulated RMS voltages are in excellent agreement with the 12.53V RMS voltages of 2010 VW Golf TDI Bluemotion EPA UDDS cycle test data. The 19.6A RMS current of the mild UDDS cycle test data is higher than 15.6A RMS current of the aggressive US06 cycle test data due approximately three times more engine stop-start events during the UDDS cycle that discharge starter motor current of approximately 220A as shown in Figure 17 and Figure 19. The charging resistances of the 92Ah lead-acid battery slightly higher because the charging voltage test data are slightly higher than the model charging voltages, although the discharging voltages from both the test data and the model simulations are very similar. Hence, lead-acid battery characteristics and performance may be different by cell chemistries, design requirements, and aging.

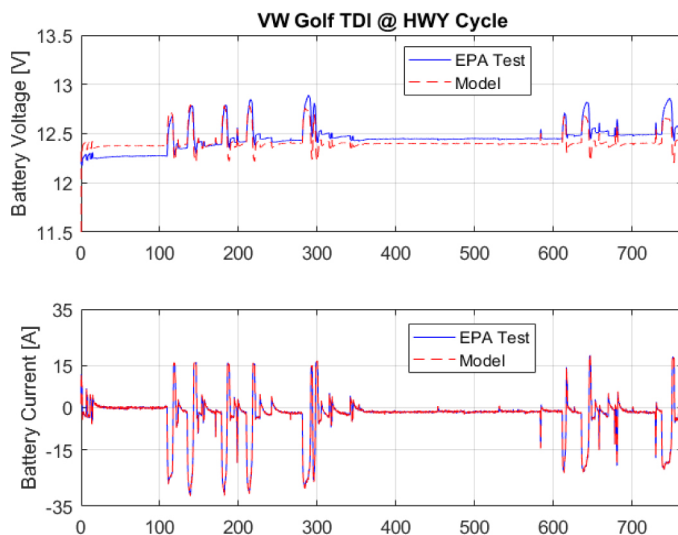


Figure 18. 2010 VW Golf TDI Highway Cycle Battery Voltages

The 12.41 V simulated RMS voltages are within 0.2% of the 12.45V RMS voltages of EPA highway cycle test data as shown in Figure 18. Charging current events are still presented although there are no engine stops during the highway driving cycle.

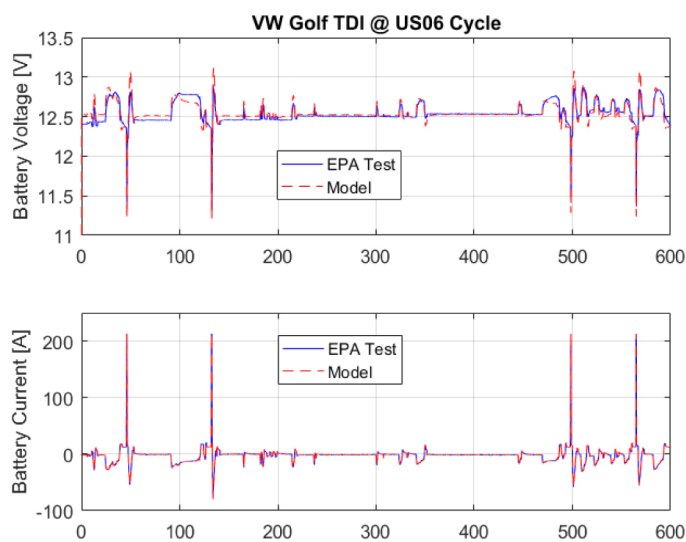


Figure 19. 2010 VW Golf TDI US06 Cycle Battery Voltages

Figure 19 shows that the 12.54V simulated RMS voltages are in excellent agreement with the 12.56V RMS voltages of 2010 VW Golf Diesel TDI Bluemotion EPA US06 cycle test data.

The battery thermal model was validated by using typical heat capacities of vented flooded and VRLA-AGM lead-acid batteries [7]. The main battery of the 2010 Mazda3 i-Stop is a 36Ah flooded lead-acid battery, and the battery weight is 7.7 kg [11].

The 1080 J/Kg-K heat capacity [7] of a typical vented flooded lead-acid battery and 0.25 W/m-K heat conductivity of an ABS plastic battery case material were input into the thermal model. The underhood temperature around the battery pack and engine bay was assumed to be 30 degrees Celsius by averaging the cabin vent temperature of ANL test data [9] when calculating heat conduction from or to the 12V lead-acid battery. The modeled RMS battery temperature of 23.52 degrees Celsius is almost identical to the 23.5 degrees Celsius found within the ANL RMS battery temperature test data. As shown in Figure 20, the battery temperature from the ANL test data and model simulations are in good agreement.

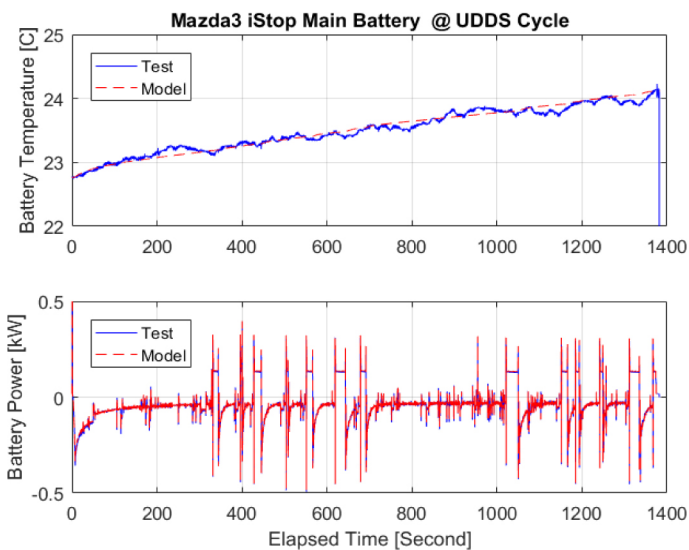


Figure 20. 2010 Mazda3 i-Stop UDDS Cycle Battery Temperature

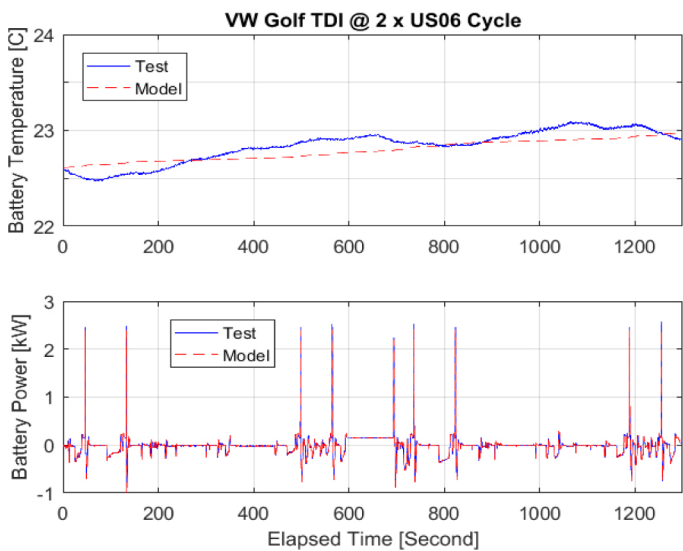


Figure 21. 2010 VW Golf TDI Battery Temperature @ 2 x US06 Cycle

The 792 J/Kg-K heat capacity [7] of a typical VRLA-AGM lead-acid battery was used for modeling the 68Ah AGM lead-acid battery of the 2010 VW Golf Diesel TDI Bluemotion. The 0.25 W/m-K heat

conductivity and 30 degrees Celsius were also used for the ABS plastic battery case and the under-hood temperature respectively. The battery temperatures increased slowly due to the 20.4Kg mass [12] of 68Ah AGM lead-acid battery although the heat capacity of the AGM lead-acid battery is smaller than that of the vented flooded lead-acid battery. The modeled RMS battery temperature of 22.81 degrees Celsius and the RMS battery temperature from US06 cycle test data of 22.84 degrees Celsius are in excellent agreement. Figure 21 shows that the battery temperature profiles of the ANL US06 cycle test data are reasonably followed by the modeled battery temperature profiles.

Conclusions

A two-time constant equivalent circuit battery cell model along with a lumped capacitance thermal model and BMS control strategies were developed and implemented in the battery pack model of the EPA ALPHA tool. The models were validated by comparison to test data and were shown to be in very good agreement. In addition, model simulation time was significantly reduced by using simple and computationally efficient models.

The look-up table based OCV, internal resistances, capacitances, RC circuit time constants and discharge/charge power limits in the battery pack model can be easily updated for the purpose of considering new lead-acid or lead-carbon battery chemistries. The number of cells in series in the battery model can be readily used for assessing 24V truck stop-start technology effectiveness by connecting two 12V batteries in series, and the battery capacity (Ampere-hour) can be extended by using the number of cells in parallel similarly for high capacity 12V lead-acid battery.

The data-driven battery pack model in the EPA ALPHA vehicle model enabled fuel economy and greenhouse gas emissions to be estimated by optimizing various battery pack design variables, SOC operating windows, power and energy densities.

The contribution of this work is the publication of resistances and capacitances of 12V lead-acid batteries, shown in the Appendix, from 10 second discharging and charging pulse tests conducted at the EPA NVFEL battery test facility (BTF), and model validation of a two-time constant equivalent circuit battery cell model and the battery thermal model [2, 5] to develop 12V Stop-Start technology effectiveness. For assessing the Stop-Start technology effectiveness, 68Ah 12V X2Power lead-acid battery test data and 92Ah 12V Duracell lead-acid battery test data were used when validating 2010 Mazda3 Hatchback i-Stop and 2010 VW Golf Diesel TDI Bluemotion drive cycle test data respectively.

References

1. Lee, S.PhD, Lee, B., Zhang, H., PhDSze, C. PhD, "Development of Greenhouse Gas Emissions Model for 2014-2017 Heavy- and Medium-Duty Vehicle Compliance," SAE Technical Paper 2011-01-2188, 2011, doi:10.4271/2011-01-2188.
2. Chen, Min and Rincon-Mora, Gabriel A., "Accurate electrical battery model capable of predicting runtime and I-V performance," IEEE Transaction on Energy Conversion, Vol. 21, No. 2, June 2006, 504-511.

3. Schweighofer, Bernhard, Raab, Klaus M., and Brasseur, Georg, "Modeling of high power automotive batteries by the use of an automated test system," IEEE Transaction on Instrumentation and Measurement, Vol. 52, No. 4, 2003.
4. Peng W., "Accurate Circuit Model for Predicting the Performance of Lead-Acid AGM Batteries." University of Nevada at Las Vegas, 2011
5. Pesaran, A.A., "Battery thermal models for hybrid vehicle simulations," Journal of Power Sources 110 (2002)
6. Pesaran, A. A., and Keyser, M., "Thermal Characteristics of Selected EV and HEV Batteries," Annual Battery Conference: Advances and Applications, Long Beach, California, January, 2001.
7. "Handbook for Stationary Lead-Acid Batteries, Part 1: Basics, Operation Modes and Applications," Handbook (part1), Industrial Power, Application Engineering Edition 6, 2012
8. Catherino, H.A, "Estimation of the heat generation rates in electrochemical cells," Journal of Power Sources 239 (2013) 505–512
9. 2010 Mazda 3 i-Stop Test Data and Reports, Argonne National Laboratory, 2011
10. 2010 VW Golf TDI Diesel Bluemotion Test Data and Reports, Argonne National Laboratory, 2011
11. 2010 Mazda 3 i-Stop – VIN1865, Advanced Vehicle Testing, Idaho National Laboratory, US Department of Energy.
12. 2010 VW Golf TDI Bluemotion – VIN8111, Advanced Vehicle Testing, Idaho National Laboratory, US Department of Energy.

Contact Information

SoDuk Lee, Ph.D.
Assessment & Standards Division
US EPA - Office of Transportation & Air Quality
2000 Traverwood Drive, Ann Arbor, MI 48105
734-214-4373
lee.soduk@epa.gov

Acknowledgments

The authors would like to acknowledge the following persons for their cooperation to this model development and validation.

Eric Rask: Argonne National Laboratory chassis dynamometer Stop-Start technology test data.

APPENDIXTable 1. R_s [mOhm], Ohmic Resistances from 92Ah Duracell PbA battery 10 second pulse tests

| Current [A] | SOC [%] with 10 second Charging Pulse Tests | | | | SOC [%] with 10 second Discharging Pulse Tests | | | |
|-------------|---|------|------|------|--|------|------|------|
| | 50 | 60 | 70 | 80 | 50 | 60 | 70 | 80 |
| 100 | 5.00 | 4.84 | 5.03 | 5.43 | 4.66 | 4.29 | 4.30 | 4.08 |
| 50 | 4.67 | 4.61 | 4.91 | 4.88 | 3.96 | 4.34 | 4.22 | 4.11 |
| 25 | 4.86 | 4.69 | 4.73 | 4.87 | 4.55 | 4.51 | 4.21 | 4.43 |
| 10 | 4.66 | 4.39 | 5.00 | 4.78 | 4.82 | 4.54 | 4.44 | 4.30 |
| 5 | 4.53 | 4.60 | 5.00 | 5.12 | 4.53 | 4.47 | 4.03 | 4.03 |

Table 2. R_{st} [mOhm], Short Time Resistances of 92Ah Duracell PbA battery in a two-time constant RC circuit

| Current [A] | SOC [%] with 10 second Charging Pulse Tests | | | | SOC [%] with 10 second Discharging Pulse Tests | | | |
|-------------|---|------|------|------|--|------|------|------|
| | 50 | 60 | 70 | 80 | 50 | 60 | 70 | 80 |
| 100 | 4.19 | 4.09 | 5.04 | 5.59 | 1.35 | 1.51 | 1.47 | 1.60 |
| 50 | 5.05 | 4.83 | 6.00 | 6.82 | 2.64 | 2.36 | 2.54 | 2.67 |
| 25 | 5.02 | 5.04 | 6.36 | 7.20 | 3.08 | 3.12 | 3.33 | 3.29 |
| 10 | 5.00 | 5.29 | 5.90 | 6.99 | 3.79 | 3.90 | 4.00 | 4.10 |
| 5 | 5.00 | 4.79 | 5.78 | 6.61 | 3.99 | 4.20 | 4.40 | 4.41 |

Table 3. R_{lt} [mOhm], Short Time Resistances of 92Ah Duracell PbA battery in a two-time constant RC circuit

| Current [A] | SOC [%] with 10 second Charging Pulse Tests | | | | SOC [%] with 10 second Discharging Pulse Tests | | | |
|-------------|---|------|------|------|--|------|------|------|
| | 50 | 60 | 70 | 80 | 50 | 60 | 70 | 80 |
| 100 | 3.13 | 2.91 | 3.78 | 4.17 | 0.92 | 1.05 | 1.03 | 1.07 |
| 50 | 3.68 | 3.58 | 4.50 | 5.00 | 1.88 | 1.72 | 1.79 | 1.85 |
| 25 | 3.86 | 3.86 | 4.75 | 5.30 | 2.32 | 2.26 | 2.48 | 2.42 |
| 10 | 3.76 | 3.74 | 4.51 | 5.21 | 2.71 | 2.84 | 2.93 | 3.09 |
| 5 | 3.71 | 3.76 | 4.40 | 5.04 | 3.12 | 3.18 | 3.08 | 3.09 |

Table 4. C_{st} [Farad], Short Time Capacitances of 92Ah Duracell PbA battery in a two-time constant RC circuit

| Current [A] | SOC [%] with 10 second Charging Pulse Tests | | | | SOC [%] with 10 second Discharging Pulse Tests | | | |
|-------------|---|-------|-------|-------|--|-------|-------|-------|
| | 50 | 60 | 70 | 80 | 50 | 60 | 70 | 80 |
| 100 | 716.0 | 660.1 | 694.5 | 697.5 | 815.1 | 662.1 | 748.4 | 750.0 |
| 50 | 713.2 | 704.1 | 666.7 | 616.2 | 530.2 | 719.2 | 708.1 | 750.2 |
| 25 | 777.0 | 773.8 | 676.2 | 624.7 | 747.2 | 800.9 | 750.2 | 881.8 |
| 10 | 759.8 | 774.8 | 712.3 | 629.7 | 843.4 | 821.2 | 824.7 | 828.8 |
| 5 | 760.2 | 772.3 | 691.7 | 635.7 | 777.4 | 714.1 | 749.8 | 793.0 |

Table 5. C_{lt} [Farad], Long Time Capacitances of 92Ah Duracell PbA battery in a two-time constant RC circuit

| Current [A] | SOC [%] with 10 second Charging Pulse Tests | | | | SOC [%] with 10 second Discharging Pulse Tests | | | |
|-------------|---|--------|--------|--------|--|--------|--------|--------|
| | 50 | 60 | 70 | 80 | 50 | 60 | 70 | 80 |
| 100 | 2201.78 | 2507.2 | 1717.9 | 1463.8 | 9685.5 | 8584.0 | 8524.6 | 8186.8 |
| 50 | 1765.72 | 1872.6 | 1357.0 | 1180.3 | 4630.4 | 4890.0 | 4700.3 | 4435.4 |
| 25 | 1604.43 | 1605.4 | 1219.9 | 1056.5 | 3365.4 | 3362.6 | 3070.2 | 2972.9 |
| 10 | 1674.53 | 1606.2 | 1284.8 | 1093.5 | 2512.4 | 2428.2 | 2323.4 | 2137.9 |
| 5 | 1671.63 | 1674.8 | 1364.1 | 1150.5 | 2210.3 | 2231.5 | 2172.2 | 2104.1 |

The Engineering Meetings Board has approved this paper for publication. It has successfully completed SAE's peer review process under the supervision of the session organizer. This process requires a minimum of three (3) reviews by industry experts.

This is a work of a Government and is not subject to copyright protection. Foreign copyrights may apply. The Government under which this paper was written assumes no liability or responsibility for the contents of this paper or the use of this paper, nor is it endorsing any manufacturers, products, or services cited herein and any trade name that may appear in the paper has been included only because it is essential to the contents of the paper.

Positions and opinions advanced in this paper are those of the author(s) and not necessarily those of SAE International. The author is solely responsible for the content of the paper.

ISSN 0148-7191

<http://papers.sae.org/2017-01-1211>